Water Air Soil Pollut (2018) 229:39
https://doi.org/10.1007/s11270-018-3693-5

Application of Novel Fulvic Acid-Coated Magnetite Nanoparticles for $CO_2^{\cdot-}$-Mediated Photoreduction of Cr(VI)

Valeria B. Arce · Carla R. Mucci · Alejandra M. Fernández Solarte · Rosa M. Torres Sánchez · Daniel O. Mártire

Received: 11 October 2017 / Accepted: 10 January 2018
© Springer International Publishing AG, part of Springer Nature 2018

Abstract We here isolate fulvic acids from vermicompost to prepare and characterize novel fulvic acid-coated magnetite nanoparticles. UV-A irradiation of suspensions of the nanoparticles under different experimental conditions led to photoreduction of Cr(VI). In anoxic conditions in the presence of formic acid, after 60 min of irradiation ca. 100% of Cr(VI) was reduced. Under these conditions, the carbon dioxide radical anions, $CO_2^{\cdot-}$, mediated the photo-reduction of Cr(VI). However, the high reduction potential of Cr(VI) and the variety of reactive species generated upon UV-A irradiation make this nanomaterial also suitable for Cr(VI) photo-reduction also under aerobic conditions in the presence of formic acid or under anoxic conditions without the addition of formic acid. The possible photodegradation routes involved are discussed in detail.

Keywords Fulvic acids · Magnetic nanoparticles · Photo-reduction · Cr(VI)

Electronic supplementary material The online version of this article (https://doi.org/10.1007/s11270-018-3693-5) contains supplementary material, which is available to authorized users.

V. B. Arce (✉)
Centro de Investigaciones Ópticas (CIOp), CONICET La Plata - CIC - UNLP, CC 3, Gonnet, 1897 La Plata, Argentina
e-mail: varce@ciop.unlp.edu.ar

C. R. Mucci · D. O. Mártire (✉)
Instituto de Investigaciones Fisicoquímicas Teóricas y Aplicadas (INIFTA), CCT-La Plata-CONICET, UNLP, Diag 113 y 64, 1900 La Plata, Argentina
e-mail: dmartire@inifta.unlp.edu.ar

A. M. Fernández Solarte · R. M. Torres Sánchez
Centro de Tecnología de recursos Minerales y Cerámica (CETMIC), CIC- CCT La Plata, Gonnet, 1897 La Plata, Argentina

A. M. Fernández Solarte
Univ. ECCI. Research group on Mechanical Design and Material (GIDMyM), Bogota DC, Colombia

1 Introduction

We have previously shown that anaerobic UV-A irradiation of 1,4-naphthoquinone (NQ) solutions containing formic acid results in the oxidation of formic acid by the triplet state of NQ to yield the carbon dioxide radical anion, $CO_2^{\cdot-}$, which reduced $HgCl_2$(aq) to Hg_2Cl_2(s) (Berkovic et al. 2012).

Humic acids (HA) and fulvic acids (FA) are operationally defined fractions of humic acids based on their solubility difference in acid and base. HA are soluble in solutions with pH > 2, whereas FA are soluble under all pH conditions (Mac Carthy 2001). The higher content of quinones in FA with respect to HA (Wu et al. 2013) motivated us toward the successful replacement of NQ with a commercial FA for the anaerobic UV-A photoreduction of $HgCl_2$ mediated by $CO_2^{\cdot-}$ (Berkovic et al. 2012).

Mixed-valence nanoscale iron oxides, such as magnetite, which present high surface areas and sorption capacities, are potential materials suitable for environmental remediation (Auffan et al. 2007).

Published online: 24 January 2018

These insoluble magnetic materials can be employed as nanoadsorbents of metal ions (Carlos et al. 2013) and organic dyes (Inbaraj and Chen, 2011) among other contaminants.

Since bare magnetite nanoparticles are susceptible to air oxidation (Maity and Agrawal 2007) and are easily aggregated in aqueous systems, their stabilization is desirable. HA-coatings enhance the stability of nanodispersions of the Fe_3O_4 particles by preventing their aggregation (Shahid et al. 2017).

On the basis of the successful employment of FA for the reduction of $HgCl_2$ and because of the convenience of using magnetic nanoparticles as carriers of FA, the aim of the present work is to synthesize and characterize novel FA-coated magnetite nanoparticles (VFANP) employing FA extracted from vermicompost (VFA). It is apparent from the above discussion that irradiation of colloidal suspensions of these nanoparticles in the presence of formic acid should generate CO_2^- radicals.

Since the most prevailing forms of chromium in the environment are Cr(VI) and Cr(III), being Cr (VI) 1000 times more toxic than Cr (III) (Shahid et al. 2017), several water treatments involving the reduction of Cr(VI) to Cr(III) have been developed. They include bioreduction (Zhang et al. 2014; Karthik et al. 2017), electrochemical reduction (Rodriguez-Valadez et al. 2005; Barrera-Díaz et al. 2011), and photocatalysis (Wang et al. 2010; Wang et al. 2016), among others. For the anaerobic photo-reduction of Cr(VI) to Cr(III), we propose here the use of VFANP, which can be easily separated and removed by applying external magnetic fields.

2 Experimental Section

2.1 Materials

$FeCl_3.3H_2O$, HCOOH, NaOH, and HCl from J.T. Baker; $FeCl_2.4H_2O$ from Merck, NaN_3 from Biopack, and NQ from Sigma–Aldrich were used without further purification. Deionized water (> 18 MΩ cm^{-1}, < 20 ppb of organic carbon) was obtained from a Millipore system.

2.2 Extraction of VFA

The fulvic acid sample (VFA) was extracted from vermicompost by a procedure proposed by Yang (Yang and Xing 2009). Briefly, a solution containing the 0.1 mol/L NaOH was mixed with vermicompost at 10:1 (v:w). The mixture was purged with N2 gas and shaken for 24 h at room temperature. The suspension was centrifuged and the supernatant was collected and acidified to pH 1, by addition of HCl, to precipitate and remove the humic acids fraction. The supernatant was adjusted to a pH of 6.0; this suspension was filtered with a membrane filter to obtain the VFA solution. The extract was dried in a rotary evaporator and then in an oven at 60 °C in vacuum.

2.3 Synthesis of Magnetic Nanoparticles

A modification of the procedure reported by Carlos (Carlos et al. 2012) for the synthesis of magnetite nanoparticles with a HA capping was used here to prepare VFANP. Briefly, 6.1706 g $FeCl_3.3H_2O$ and 3.0185 g $FeCl_2.4H_2O$ were dissolved in water and heated to 90 °C. Then, two aqueous solutions were added rapidly and sequentially: (1) 10 mL of 25% ammonium hydroxide and (2) 50 mL of 1.0% *w/v* VFA. The mixture was stirred at 90 °C for 30 min and then cooled to room temperature. The product was filtered through an HPLC filtration device with 20-nm-nylon filters, washed with water, then was dried at 60 °C for 5 h in vacuum. The black precipitate obtained was stored at room temperature as a dry black powder prior to use in the experiments.

The nanoparticles were characterized by Fourier transform infrared spectroscopy (FTIR), total organic carbon (TOC), electron microscopy (SEM), Brunauer–Emmett–Teller analysis (BET), thermal gravimetric analysis (TGA), zeta potential (ζ), dynamic light scattering (DLS), and magnetization. Characterization techniques and instrumentation are described in the supplementary material.

2.4 Steady-State Irradiation Experiments

Ar-saturated colloidal suspensions of VFANP containing formic acid were irradiated in a Rayonet RPR-100 reactor equipped with eight RPR-3500 lamps. The samples were contained in 25-mL glass tubes.

After irradiation the nanoparticles were separated with the aid of a magnet. The assays were performed at pH = 2, where the main species of Cr(VI) is $Cr_2O_7^{2-}$ and its concentration was followed by UV-visible

spectroscopy ($\varepsilon^{346} = 3112\ M^{-1}\ cm^{-1}$) (Kumagai et al. 2011). All the experiments were performed by triplicate.

3 Results and Discussion

3.1 Characterization of VFA

Figure 1 shows the ATR transmittance spectrum of VFA. The highest absorption band at around 3400 cm^{-1} is assigned to the O–H stretching of carboxylic acids, phenols, and alcohols. The bands around 2920–2850 cm^{-1} are characteristics of the aliphatic C–H stretching (Andjelkovic et al. 2006; Martín et al. 2014). Bands at around 1350 and 1600 cm^{-1} are due to C=O stretches. The broad band at 1100–1000 cm^{-1} present only in the extract is characteristic of aromatic ethers and polysaccharides (Amir et al. 2003). The sharp band below 700 cm^{-1} corresponds to Fe–O stretching vibration, which is centered at ~ 630 cm^{-1} (Carlos et al. 2012).

From the C content of the VFA (9.80%) as determined by TOC analysis and the UV-visible absorption spectrum (Fig. 2a), the molar absorptivity at 280 nm per mole of organic carbon $\varepsilon^{280} = 119.5\ L\ mol_{CO}^{-1}.cm^{-1}$ was obtained. This is a useful parameter for the estimation of an operational molecular weight of humic substances MW. From the linear correlation between ε^{280} and MW, a value of MW = 967 Da is obtained (Chin et al. 1994). The absorbance ratio at two different wavelengths in the visible region, 465 and 665 nm (namely E4/E6 ratio), has been long considered to inversely correlate with the molecular size and/or the formation

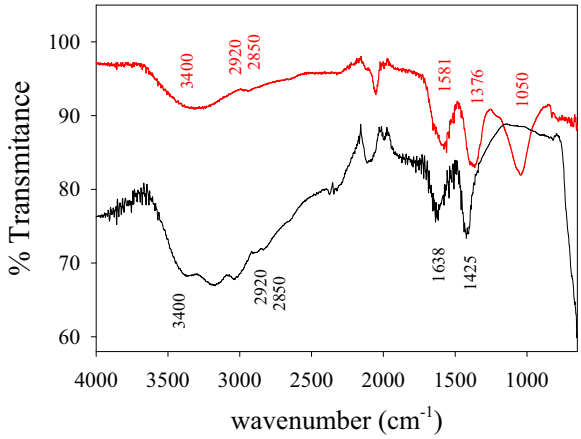

Fig. 1 ATR spectra of the VFA (upper trace) and VFANP (lower trace)

of multiring aromatic systems in humic substances (Uyguner and Bekbolet 2005). The values of $\varepsilon^{280} = 119.5\ L\ mol_{CO}^{-1}.cm^{-1}$, molecular weight (MW) = 967 Da, and E4/E6 = 3.30 obtained here for VFA are all in complete agreement with those reported for other fulvic acids (Chin et al. 1994).

The excitation-emission maxima pair ($\lambda^{ex}/\lambda^{em}$) of the EEM of VFA is placed at 330/430 nm (Fig. 2b). These values are in excellent agreement with those reported for fulvic acids (http://www.humicsubstances.org/spectra.html).

3.2 Characterization of VFANP

The results of VFANP characterization are summarized in Table 1. SEM images of VFANP show that the average nanoparticle size is (13.2 ± 0.3) nm (Fig. 3). The specific surface area (S_{BET}) was (84 ± 4) $m^2\ g^{-1}$.

The absorption at 650 cm^{-1} present in the ATR spectrum of VFANP (Fig. 1) confirms the presence of magnetite in the samples (Carlos et al. 2012). Significant differences in the bands assigned to C=O stretches at around 1400 and 1600 cm^{-1} are indicative of the interaction between carboxylate anions of VFA with the FeO surface, as observed for magnetite nanoparticles coated with dimercaptosuccinic and humic acids (Carlos et al. 2012; Yantasee et al. 2007; Liu et al. 2008).

Figure 4a shows the DTA-TGA curves of nanoparticles. The TGA curve exhibits a constant mass loss from ambient temperature to 800 °C. The endothermic peak width accompanied by a significant mass loss, below 200 °C, in DTA curve corresponding to desorption of physisorbed water in the sample. The exothermic peak at 430 °C is attributed to decomposition of fulvic acid present on the surface of the nanoparticle. This peak indicates the formation of Fe-FA complex, since the decomposition of fulvic acid cores without metallic bonds takes place at a higher temperature (about 450 °C). Finally, the exothermic peak at 630 °C assigned to a possible transition phase magnetite-hematite (Chen 2013) or a possible reduction of Fe_3O_4 to FeO (Schnitzer and Kodama 1971).

The pH dependence of the zeta potential (ζ) of VFANP dispersions in 10^{-3} M KCl aqueous solutions shows a pH of zero point charge (pH_{PZC}) of 5.7 (Fig. 4b). The shift of the pH_{PZC} value with respect to the underivatized magnetite nanoparticles ($pH_{PZC} = 6.7$) (Chang and Chen 2005) confirms the coverage with the organic material, since the VFA is negatively

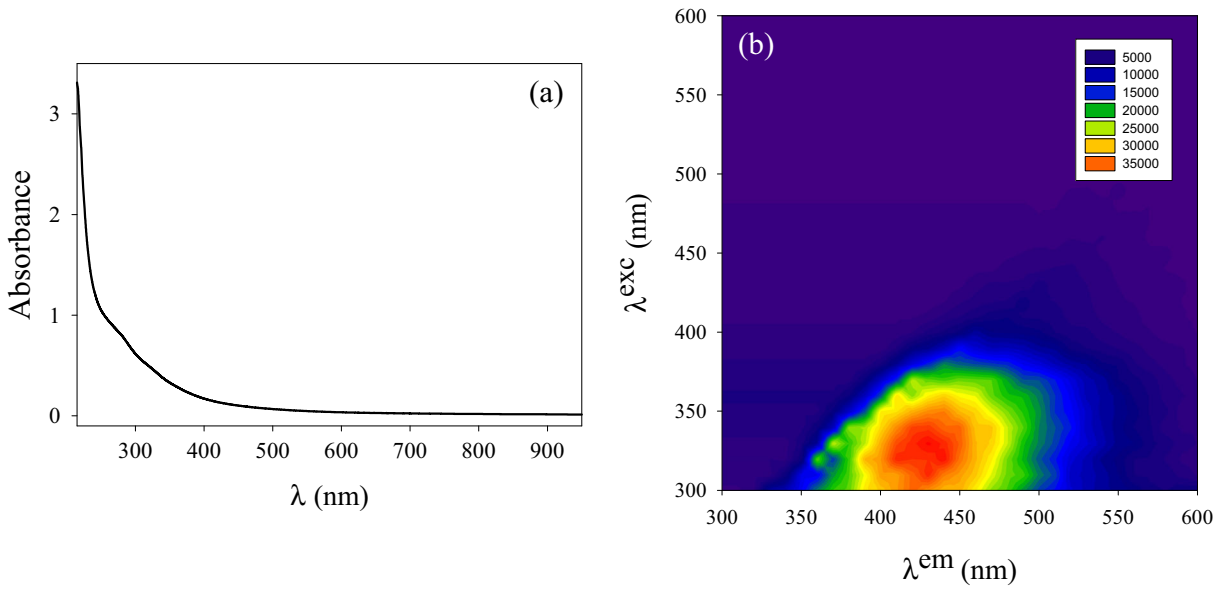

Fig. 2 **a** UV-visible spectrum of a 0.82 g L^{-1} solution of VFA at pH = 7. **b** Excitation-emission matrix of VFA

charged in the whole pH range due to the deprotonation of carboxylic and phenolic groups (Fig. 4b).

The apparent diameter of the nanoparticles obtained from DLS measurements performed with 1 mg mL^{-1} of VFANP suspensions at pH = 4.5 ± 0.2 was 206.6 ± 1.9 and 1062.4 ± 70.6 nm in water and 2.10 M KCl, respectively. Thus, the aggregation is favored at high ionic strength, as expected from the reduction of the thickness of the electric double layer and repulsive forces under this condition (Hotze et al. 2010).

The magnetization curves of VFANP and Fe_3O_4 at 300 K (Fig. 5) show superparamagnetic behavior, including zero coercivity (H_c) and remanence (M_r) (Luo et al. 2014). The saturation magnetization (M_s) of the underivatized magnetite nanoparticles and VFANP were 65.256 and 60.892 emu g^{-1}, respectively. The decrease of M_s upon derivatization of magnetite with organic coatings was previously observed (Sun et al. 2009; Magnacca et al. 2014) and was assigned to quenching of surface moments, resulting in the reduction of magnetic moment in the coated particles (Kim et al. 2003).

3.3 Steady-State Irradiation Experiments

Ar-saturated aqueous colloidal suspensions of 2 g L^{-1} VFANP (pH = 2) containing 0.4 M formic acid, and 0.1 mM $K_2Cr_2O_7$ were irradiated at 350 nm (eight lamps). The decay of the $Cr_2O_7^{2-}$ concentration upon irradiation follows a first order kinetics with an apparent rate constant of 0.057 min^{-1} (Fig. 6a).

As can be seen in Fig. 6, after 60 min of irradiation ca. a 100% removal of $Cr_2O_7^{2-}$ is achieved. Under the conditions of these experiments the triplet excited states of FA (^{3}FA*) react with HCOOH to yield CO_2^- radicals.[1] Additionally, photolysis of FA leads to the generation of low amounts of hydroxyl

Table 1 Results of VFANP characterization

Techniques	Parameters	Results
SEM	Average diameter (nm)	13.2 ± 0.3
TGA	FA adsorbed to Fe_3O_4 (%)	5
BET	S_{BET} (m^2 g^{-1})	84 ± 4
DLS	Average hydrodynamic diameter (nm)	206.6 ± 1.9 (water) 1062.4 ± 70.6 (2.10 M KCl)
Magnetization (M_s)	Saturation magnetization (emu g^{-1})	60.892

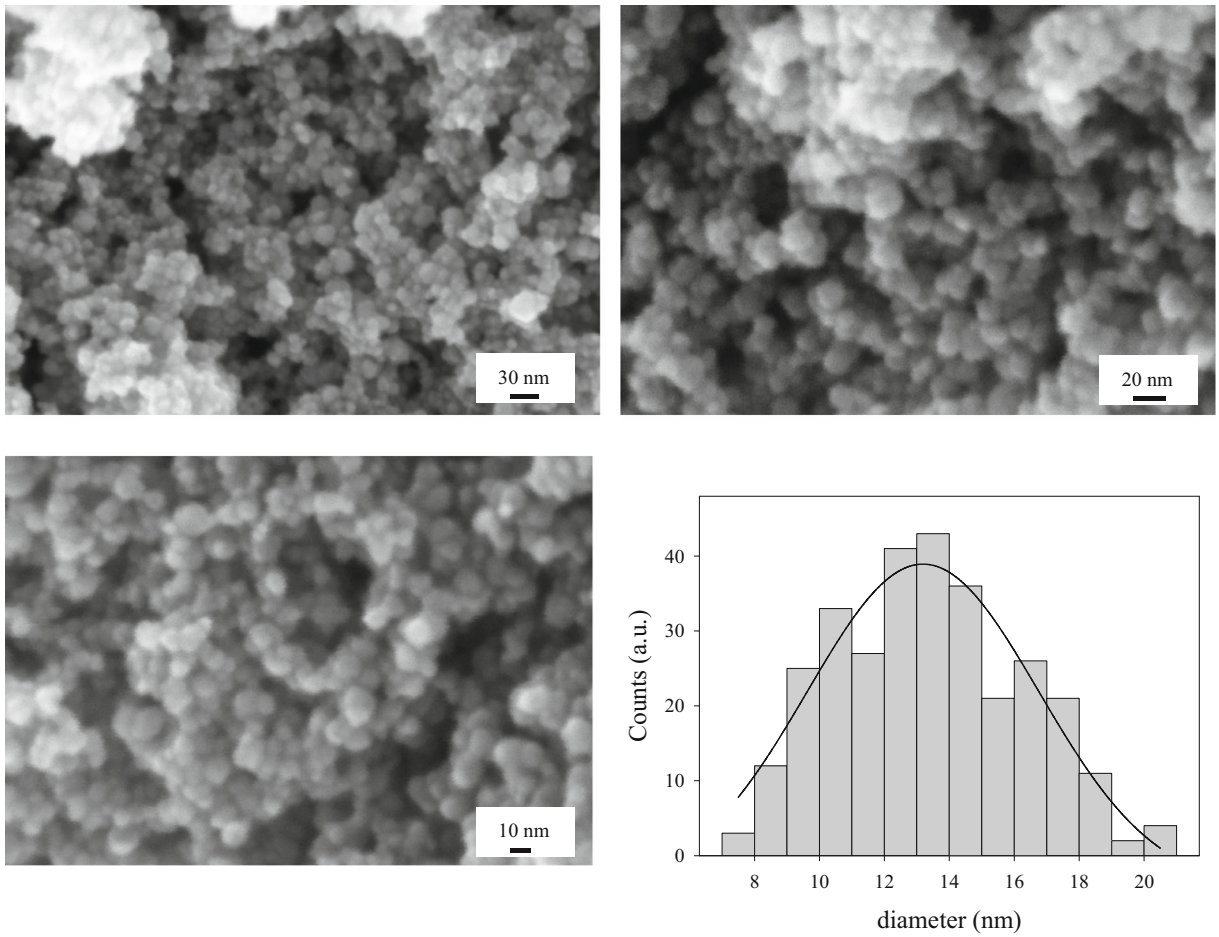

Fig. 3 SEM images and histogram from VFANP

radicals (Vaughan and Blough 1998) and these oxidative species also scavenged the yield of $CO_2^{\cdot-}$ radicals (David Gara et al. 2007). These radicals are able to reduce $Cr_2O_7^{2-}$ to Cr^{3+} according to reaction 3 (Ren et al. 2017) (see reduction potentials in Table 2).

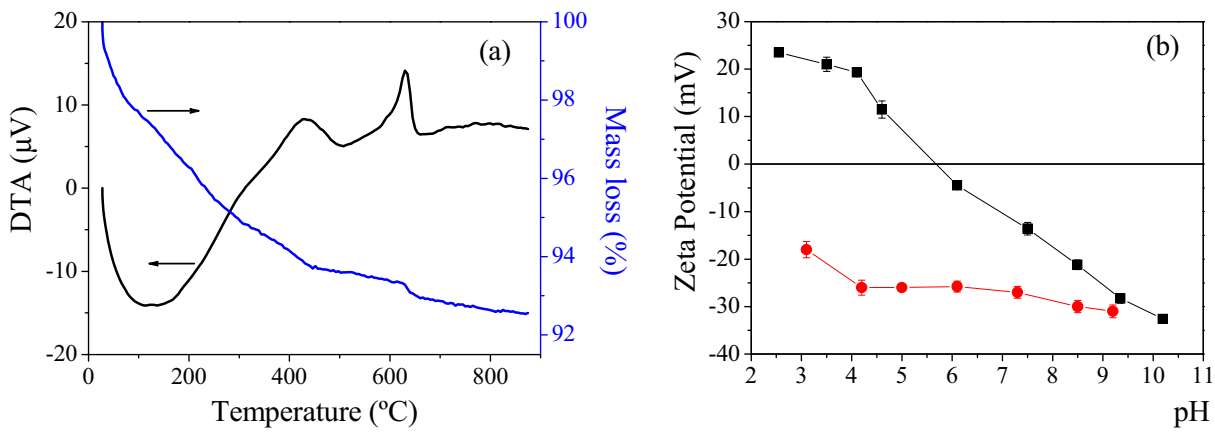

Fig. 4 **a** DTA (black) and TGA (blue) curves obtained for VFANP. **b** pH-dependence of zeta potential (ζ) for VFANP (black) and VFA (red) in 0.001 M KCl medium

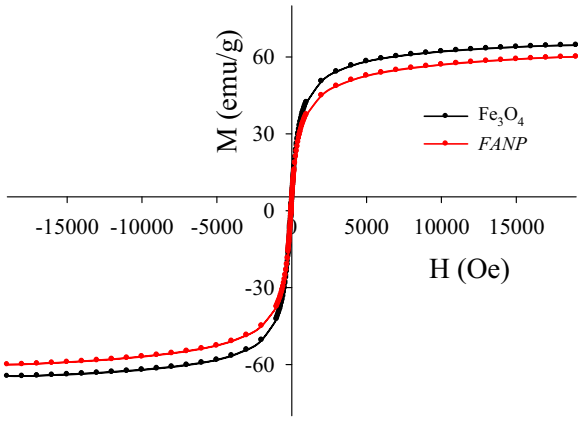

Fig. 5 Magnetization curves of Fe_3O_4 and VFANP

$$6\ CO_2^{\cdot-} + Cr_2O_7^{2-} + 14\ H^+ \rightarrow 2\ Cr^{3+} + 7\ H_2O + 6\ CO_2 \quad (3)$$

Moreover, according to the strength as reducing agents of some of the triplet states of humic substances estimated by McNeill and Canonica (McNeill and Canonica 2016) (see reduction potential in Table 2), these excited states as well as charge-transfer states (Zhang and Blough, 2016) can also reduce Cr(VI).

Near-UV/visible photoionization of humic substances is known to generate solvated electrons and radical cations of phenolic groups, which rapidly deprotonate to yield phenoxyl radicals (Martin et al. 2017). The reduction of $Cr_2O_7^{2-}$ to Cr^{3+} by solvated electrons and phenoxyl radicals is also thermodynamically feasible (Table 2), and thus these reaction could also contribute to the efficient photodegradation of Cr(VI). Even hydrogen peroxide (Zhang and Blough, 2016) could act as reducing agent (Table 2).

Table 2 Literature redox potentials

Redox couple	*E*/V
$Cr_2O_7^{2-}/Cr^{3+}$	1.33[a, b]
CO_2/CO_2^{-}	−1.9[a, c]
aq/e^-_{aq}	−2.87[a, c]
O_2/O_2^{-}	−0.18[a, d]
$O_2/HO_2^{\cdot}$ (pH = 0)	−0.037[c]
$PhO^{\cdot}/PhOH$	1.3[e]
$FA^{\cdot+}/^3FA^*$	−0.60 < E < −0.18[f]
O_2/H_2O_2	0.28[d]

The values were estimated from data obtained with chromophoric dissolved organic matter

[a] Standard potentials

[b] From Wang et al. 2008

[c] From Wardman 1989

[d] From Koppenol et al. 2010

[e] From Li and Hoffman 1999

[f] From McNeill and Canonica 2016

Comparative experiments under air-saturation showed only a 46% degradation of Cr(VI) (Fig. 6). Under these conditions the routes of Cr(VI) reduction involving phenoxyl and hydroxyl radicals (see above) and hydrogen peroxide, are still operative. But the triplet

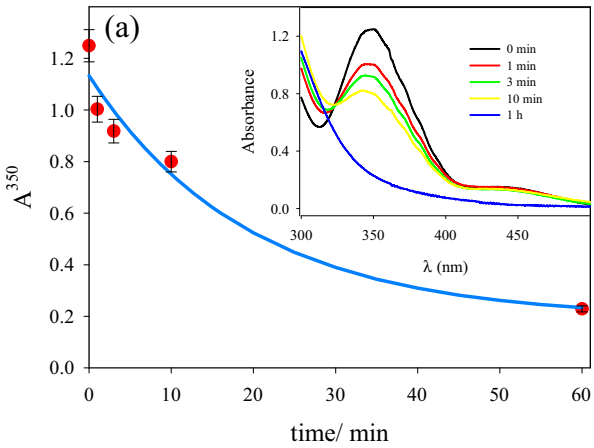

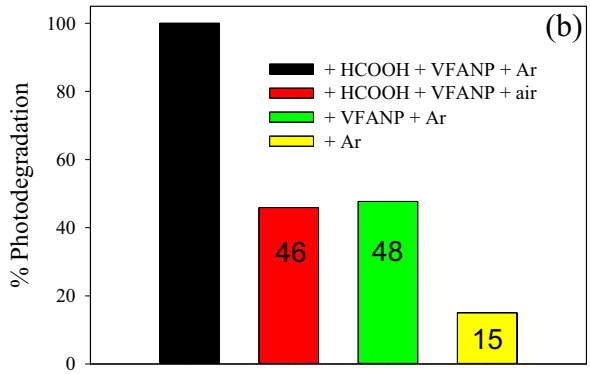

Fig. 6 **a** Time evolution of $Cr_2O_7^{2-}$ concentration upon irradiation of an Ar-saturated 0.1 mM solution of $Cr_2O_7^{2-}$ in the presence of 2 g L^{-1} VFANP and 0.4 M HCOOH. The error bars represent standard deviations. Inset shows UV-visible spectra of the solutions obtained after removing the nnaoparticles with a magnet. **b** Percentage of photodegradation after 60 min irradiation of different samples as indicated

states of FA are mainly quenched to yield the oxidizing species singlet oxygen (Carlos et al. 2012), and the CO_2^- radicals and solvated electrons are scavenged by O_2 to yield O_2^- (David Gara et al. 2007; http://kinetics.nist.gov/solution/). From the acid dissociation constant (pKa ~ 4.8) (Bielski et al. 1985), at pH 2 the superoxide radical anion will be mainly protonated. The observed reduction of Cr(VI) (Fig. 6) could be mediated by both $HO_2^{\cdot}$ and O_2^- (see redox potentials in Table 2).

Experiments performed under Ar-saturation in the presence of VFANP but without formic acid showed a 48% degradation of Cr(VI) (Fig. 6). In the absence of HCOOH, CO_2^- is not formed but triplet states, phenoxyl radicals and solvated electrons could be responsible for the reduction of Cr(VI).

Blank irradiation experiments performed with Ar-saturated $K_2Cr_2O_7$ solutions without nanoparticles and formic acid for 60 min showed only a 15% Cr(VI) consumption (Fig. 6b), indicating that the contribution of direct photolysis is a minor photodegradation route. Blank experiments in the dark during the same period revealed no $Cr_2O_7^{2-}$ consumption, in line with the reported slow reduction of Cr(VI) by FA (Wittbrodt and Palmer 1995).

4 Conclusion

We here clearly demonstrate that FA can be easily transformed into a magnetic additive for the photochemical treatment of water contaminated with Cr(VI).

The high reduction potential of Cr(VI) and the variety of reactive species generated upon UV-A irradiation make this nanomaterial suitable for Cr(VI) photoreduction under several conditions. The best performances were obtained under Ar-saturation and in the presence of formic acid. However, albeit with a lower efficiency, the nanomaterials also photosensitize the reduction of Cr(VI) either under aerobic conditions in the presence of formic acid or under anoxic conditions without the addition of formic acid. The possible photodegradation routes involved are discussed in deeply.

The photochemical treatment described here involves the use of UV-A light, which is in the region of the electromagnetic spectrum (320–400 nm) within the solar radiation reaching the Earth's surface. Thus, the procedure could be useful for Cr(VI) reduction in aqueous systems because solar radiation could be employed as light source and the nanomaterials could be easily removed by application of an external magnetic field.

Acknowledgements V.B.A. and D.O.M. are researchers from Comisión de Investigaciones Científicas de la Provincia de Buenos Aires. R.M.T.S. is researcher from CONICET.

Funding Information This work was supported by Grant PICT 2012 # 1817 from Agencia Nacional de Promoción Científica y Tecnológica, (ANPCyT, Argentina).

References

Amir, S., Hafidi, M., Bailly, J.-R., & Revel, J.-C. (2003). Characterization of humic acids extracted from sewage sludge during composting and of their Sephadex® gel fractions. *Agronomie, 23*, 269–275.

Andjelkovic, T., Perovic, J., Purenovic, M., Blagojevic, S., Nikolic, R., Andjelkovic, D., & Bojic, A. (2006). Spectroscopic and potentiometric studies on derivatized natural humic acid. *Analytical Sciences, 22*, 1553–1558.

Auffan, M., Shipley, H. J., Yean, S., Kan, A. T., Tomson, M., Rose, J., & Bottero, J. Y. (2007). Nanomaterials as adsobents. In M. R. Wiesner & J. Y. Bottero (Eds.), *Environmental nanotechnology: applications and impacts of nanomaterials*. New York: McGraw-Hill.

Barrera-Díaz, C., Lugo-Lugo, V., Roa-Morales, G., Natividad, R., & Martínez-Delgadillo, S. A. (2011). Enhancing the electrochemical Cr(VI) reduction in aqueous solution. *Journal of Hazardous Materials, 185*, 1362–1368.

Berkovic, A. M., Bertolotti, S. G., Villata, L. S., Gonzalez, M. C., Pis Diez, R., & Mártire, D. O. (2012). Photoinduced reduction of divalent mercury by quinones in the presence of formic acid under anaerobic conditions. *Chemosphere, 89*, 1189–1194.

Bielski, B. H. J., Cabelli, D. E., Arudi, R. L., & Ross, A. B. (1985). Reactivity of $HO_2/O_2^{\cdot}$ radicals in aqueous solution. *Journal of Physical and Chemical Reference Data, 14*, 1041–1100.

Carlos, L., Cipollone, M., Soria, D. B., Moreno, S., Ogilby, P. R., García Einschlag, F. S., & Mártire, D. O. (2012). The effect of humic acid binding to magnetite nanoparticles on the photogeneration of reactive oxygen species. *Separation and Purification Technology, 91*, 23–29.

Carlos, L., García Einschlag, F. S., Gonzalez, M. C., & Mártire, D. O. (2013). Applications of magnetite nanoparticles for heavy metal removal from wastewater. In F. S. García Einschlag & L. Carlos (Eds.), *Waste water-treatment technologies and recent analytical developments*. Intech-Open Access Publisher. https://doi.org/10.5772/54608

Chang, Y. C., & Chen, D. H. (2005). Preparation and adsorption properties of monodisperse chitosan-bound Fe_3O_4 magnetic nanoparticles for removal of Cu(II) ions. *Journal of Colloid and Interface Science, 283*, 446–451.

Chen, Y. H. (2013). Thermal properties of nanocrystalline goethite, magnetite, and maghemite. *Journal of Alloys and Compounds, 553*, 194–198.

Chin, Y. P., Aiken, G., & O'Loughlin, E. (1994). Molecular weight, polydispersity and spectroscopic properties of aquatic humic substances. *Environmental Science & Technology, 28*, 1853–1858.

David Gara, P., Bucharsky, E., Wörner, M., Braun, A. M., Mártire, D. O., & Gonzalez, M. C. (2007). Trichloroacetic acid dehalogenation by reductive radicals. *Inorganica Chimica Acta, 360*, 1209–1216.

Hotze, E. M., Phenrat, T., & Lowry, G. V. (2010). Nanoparticle aggregation: challenges to understanding transport and reactivity in the environment. *Journal of Environmental Quality, 39*, 1909–1924 http://www.humicsubstances.org/spectra.html

Inbaraj, B. S., & Chen, B. H. (2011). Dye adsorption characteristics of magnetite nanoparticles coated with a biopolymer poly(γ-glutamic acid). *Bioresource Technology, 102*, 8868–8876.

Karthik, C., Barathi, S., Pugazhendhi, A., Ramkumar, V. S., & Arulselvi, P. I. (2017). Evaluation of Cr(VI) reduction mechanism and removal by cellulosimicrobium funkei strain AR8, a novel haloalkaliphilic bacterium. *Journal of Hazardous Materials, 333*, 42–53.

Kim, D. K., Mikhaylova, M., Zhang, Y., & Muhammed, M. (2003). Protective coating of superparamagnetic iron oxide nanoparticles. *Chemistry of Materials, 15*, 1617–1627.

Koppenol, W. H., Stanbury, D. M., & Bounds, P. L. (2010). Bounds, electrode potentials of partially reduced oxygen species, from dioxygen to water. *Free Radical Biology & Medicine, 49*, 317–322.

Kumagai, Y., Nagaishi, R., Yamada, R., & Katsumura, Y. (2011). Effect of silica gel on radiation-induced reduction of dichromate ion in aqueous acidic solution. *Radiation Physics and Chemistry, 80*, 876–883.

Li, C., & Hoffman, M. Z. (1999). One-electron redox potentials of phenols in aqueous solution. *The Journal of Physical Chemistry. B, 103*, 6653–6656.

Liu, J. F., Zhao, Z. S., & Jiang, G. B. (2008). Coating Fe_3O_4 magnetic nanoparticles with humic acid for high efficient removal of heavy metals in water. *Environmental Science & Technology, 72*, 6949–6954.

Luo, W., Ma, H., Mou, F., Zhu, M., Yan, J., & Guan, J. (2014). Steric-repulsion-based magnetically responsive photonic crystals. *Advanced Materials, 26*, 1058–1064.

Mac Carthy, P. (2001). The principles of humic substances: an introduction to the first principle. In A. A. Ghabbour & G. Davies (Eds.), *Humic substances. structures, models and functions*. Gateshead: The Royal Society of Chemistry.

Magnacca, G., Allera, A., Montoneri, E., Celi, L., Benito, D., Gagliardi, L., Gonzalez, M., Mártire, D., & Carlos, L. (2014). Novel magnetite nanoparticles coated with waste sourced bio-based substances as sustainable and renewable adsorbing materials. *ACS Sustainable Chemistry & Engineering, 2*, 1518–1524.

Maity, D., & Agrawal, D. C. (2007). Synthesis of iron oxide nanoparticles under oxidizing environment and their stabilization in aqueous and non-aqueous media. *Journal of Magnetism and Magnetic Materials, 308*, 46–55.

Martín, M. V., Gebühr, C., & Mártire, D. O. (2014). Characterization of a humic acid extracted from marine sediment and its influence on the growth of marine diatoms. *Journal of the Marine Biological Association of the UK, 94*, 895–906.

Martin, M. V., Mignone, R. A., Rosso, J. A., David Gara, P., Pis Diez, R., Borsarelli, C. D., & Mártire, D. O. (2017). Transient spectroscopic characterization and theoretical modeling of fulvic acid radicals formed by UV-A radiation. *Journal of Photochemistry and Photobiology A: Chemistry, 332*, 571–579.

McNeill, K., & Canonica, S. (2016). Triplet state dissolved organic matter in aquatic photochemistry: Reaction mechanisms, substrate scope, and photophysical properties. *Environmental Science: Processes & Impacts, 18*, 1381–1399.

NDRL/NIST. (2002). Solution kinetics database on the web. Available on the web at: http://kinetics.nist.gov/solution/.

Ren, H., Hou, Z., Han, X., & Zhou, R. (2017). Highly reductive radical $CO_2^{\cdot-}$ deriving from a system with $SO_4^{\cdot-}$ and formate anion: implication for reduction of Cr(VI) from wastewater. *Chemical Engineering Journal, 309*, 638–645.

Rodriguez-Valadez, F., Ortiz-Éxiga, C., Ibanez, J. G., Alatorre-Ordaz, A., & Gutierrez-Granados, S. (2005). Electroreduction of Cr(VI) to Cr(III) on reticulated vitreous carbon electrodes in a parallel-plate reactor with recirculation. *Environmental Science & Technology, 39*, 1875–1879.

Shahid, M., Shamshad, S., Rafiq, M., Khalid, S., Bibi, I., Niazi, N. K., Dumat, C., & Rashid, M. I. (2017). Chromium speciation, bioavailability, uptake, toxicity and detoxification in soil-plant system: a review. *Chemosphere, 78*, 513–533.

Schnitzer, M., & Kodama, H. (1971). Differential thermal analysis of metal-fulvic acid salts and complexes. *Geoderma, 7*, 93–103.

Sun, X., Zheng, C., Zhang, F., Yang, Y., Wu, G., Yu, A., & Guan, N. (2009). Size-controlled synthesis of magnetite (Fe_3O_4) nanoparticles coated with glucose and gluconic acid from a single Fe(III) precursor by a sucrose bifunctional hydrothermal method. *Journal of Physical Chemistry C, 113*, 16002–16008.

Uyguner, C. S., & Bekbolet, M. (2005). Implementation of spectroscopic parameters for practical monitoring of natural organic matter. *Desalination, 176*, 47–55.

Vaughan, P. P., & Blough, N. V. (1998). Photochemical formation of hydroxyl radical by constituents of natural waters. *Environmental Science & Technology, 32*, 2947–2953.

Wang, N., Zhu, L., Deng, K., She, Y., Yu, Y., & Tang, H. (2010). Visible light photocatalytic reduction of Cr(VI) on TiO2 in situ modified with small molecular weight organic acids. *Applied Catalysis B: Environmental*, 400–407.

Wang, J. C., Ren, J., Yao, H. C., Zhang, L., Wang, J. S., Zang, S. Q., Han, L. F., & Li, Z. J. (2016). Synergistic photocatalysis of Cr(VI) reduction and 4-chlorophenol degradation over hydroxylated α-Fe_2O_3 under visible light irradiation. *Journal of Hazardous Materials, 311*, 11–19.

Wang, G., Huang, L., & Zhang, Y. (2008). Cathodic reduction of hexavalent chromium [Cr(VI)] coupled with electricity generation in microbial fuel cells. *Biotechnology Letters, 30*, 1959–1966.

Wardman, P. (1989). Reduction potentials of one-electron couples involving free radicals in aqueous solution. *Journal of Physical and Chemical Reference Data, 18*, 1637–1755.

Wittbrodt, P. R., & Palmer, C. D. (1995). Reduction of Cr(VI) in the presence of excess soil fulvic acid. *Environmental Science & Technology, 29*, 255–263.

Wu, C. Y., Zhuang, L., Zhou, S. G., Yuan, Y., Yuan, T., & Li, F. B. (2013). Humic substance-mediated reduction of iron(III) oxides and degradation of 2,4-D by an alkaliphilic bacterium, Corynebacterium humireducens MFC-5. *Microbial Biotechnology, 6*, 141–149.

Yang, K., & Xing, B. (2009). Adsorption of fulvic acid by carbon nanotubes from water. *Environmental Pollution, 157*, 1095–1100.

Yantasee, W., Warner, C. L., Sangvanich, T., Addleman, R. S., Carter, T. G., Wiacek, R. J., Fryxell, G. E., Timchalk, C., & Warner, M. G. (2007). Removal of heavy metals from aqueous systems with thiol functionalized superparamagnetic nanoparticles. *Environmental Science & Technology, 41*, 5114–5119.

Zhang, Y., & Blough, N. V. (2016). Photoproduction of one-electron reducing intermediates by chromophoric dissolved organic matter (CDOM): relation to $O_2^{\cdot-}$ and H_2O_2 photoproduction and CDOM photooxidation. *Environmental Science & Technology, 50*, 11008–11015.

Zhang, H. K., Lu, H., Wang, J., Zhou, J. T., & Sui, M. (2014). Cr(VI) reduction and Cr(III) immobilization by Acinetobacter sp. HK-1 with the assistance of a novel quinone/graphene oxide composite. *Environmental Science & Technology, 48*, 12876–12885.